

https://doi.org/10.1070/QEL16201

A factor limiting the accuracy of optical loss measurements in single-mode fibres: 'frozen-in' inhomogeneities of the Rayleigh backscatter coefficient

V.I. Busurin, B.G. Gorshkov, G.B. Gorshkov, M.L. Grinshtein, M.A. Taranov

Abstract. **Backscatter coefficient fluctuations at a wavelength of 1560 nm in Fujikura FutureGuide-LWP, Corning ClearCurve XB and Corning SMF-28 ULL telecom fibres have been studied using optical time-domain reflectometry and broadband (10 nm) depolarised light. It has been shown that, under the conditions of our experiments, such fluctuations are 'frozen-in' and that a typical standard deviation in noiselike reflectograms is 0.16 dB, with a correlation distance no greater than 1 m. Such results have been obtained for all fibre samples. The effect studied experimentally limits the accuracy of attenuation measurements in optical fibres, especially at short fibre lengths (tens and hundreds of metres). Moreover, it should be taken into account in designing distributed physical parameter sensors using Rayleigh scattering intensity as a reference channel. Possible sources of the inhomogeneities in the fibres are discussed.**

Keywords: *optical reflectometry, optical fibres, Rayleigh scattering.*

1. Introduction

Optical reflectometry is a key method for loss measurements in optical fibres and is widely used in making distributed physical parameter sensors. If the parameter to be monitored is Rayleigh scattering intensity, the metrological properties of instruments are better at a lower noise level in reflectograms. In particular, in loss (dB km^{-1}) measurements, noise makes accurate loss assessment impossible at short fibre lengths (tens and hundreds of metres).

In designing distributed temperature sensors based on Raman scattering intensity measurements, it is reasonable to use a Rayleigh scattering reflectogram as a reference channel [1]. However, the noisiness observed by us in Rayleigh scattering reflectograms, which cannot be eliminated by increasing the signal acquisition time, introduces noise corresponding to a temperature of at least 0.5–1.0 K into the measured temperature profile. Because of this, understanding mechanisms underlying such behaviour of Rayleigh scattering reflectograms is of current interest and practical importance.

Two mechanisms are known to be responsible for the noise contamination of Rayleigh scattering reflectograms. One of them is related to polarisation effects [2, 3]. A light source (usually, a laser diode) typically produces linearly polarised light, whose polarisation state varies arbitrarily during propagation through a non-polarisation-maintaining fibre. Scattering of light does not change its polarisation state, and the backscattered light travels to a photodetector through formally polarisation-insensitive components (coupler or circulator). Nevertheless, these components introduce polarisation-dependent losses, typically in the range 0.03 to 0.2 dB, producing polarisation noise.

The use of various known depolarisation methods (averaging over the spectrum and time averaging, i.e. scrambling) allows one to essentially eliminate polarisation noise.

The other mechanism is coherence noise. It originates from random interference of scattered waves when probe light has a sufficiently narrow bandwidth. The presence of a noiselike component in a reflectogram underlies phase-sensitive reflectometry [4, 5] but is a problem in designing reflectometers for loss measurements in optical fibres. Attempts to eliminate such noise reduce to either extending the source spectrum or scanning (sweeping) its centre frequency in the course of measurements. This noise source can in principle be also essentially eliminated. There is, however, a third mechanism, which has been identified and investigated in this study. This mechanism is related to the properties of optical fibres, namely, to the longitudinal inhomogeneity of their physical properties.

2. Experimental setup and discussion of results

In our experiments, we used the setup schematised in Fig. 1.

The master oscillator used was a Superlum SLD 761 superluminescent diode. Its output was amplified by a two-stage erbium-doped fibre amplifier. The pulse duration was 5 ns, the pulse shape was nearly Gaussian, and the pulse bandwidth after the amplifier was about 10 nm. The probe light had a centre wavelength of 1.56 μm, peak power within 1 W and pulse repetition rate up to 200 kHz. The light source was followed by a fibre-optic Lyot depolariser (Phoenix Photonics, Model DPOL-BB-15-SS). Thus, all measures were taken to obtain broadband depolarised light. After passing through a circulator with a rated polarisation-dependent loss of 0.09 dB and through a 105-m-long dummy fibre spool, the light entered Fujikura FutureGuide-LWP, Corning ClearCurve XB and Corning SMF-28 ULL optical

V.I. Busurin Moscow Aviation Institute (National Research University), Volokolamskoe sh. 4, Moscow, 125993 Russia;
B.G. Gorshkov A.M. Prokhorov General Physics Institute, Russian Academy of Sciences, ul. Vavilova 38, 119991 Moscow, Russia;
G.B. Gorshkov, M.A. Taranov OOO Petrofaiber, Klinskii proezd 7, 301664 Novomoskovsk, Tula region, Russia;
e-mail: gorgb@petrofibre.ru;
M.L. Grinshtein ZAO Institute of Information Technologies, Oktyabr'skaya ul. 19/5, 220030 Minsk, Belarus

Received 24 August 2016; revision received 19 October 2016
Kvantovaya Elektronika **47** (1) 83–86 (2017)
Translated by O.M. Tsarev

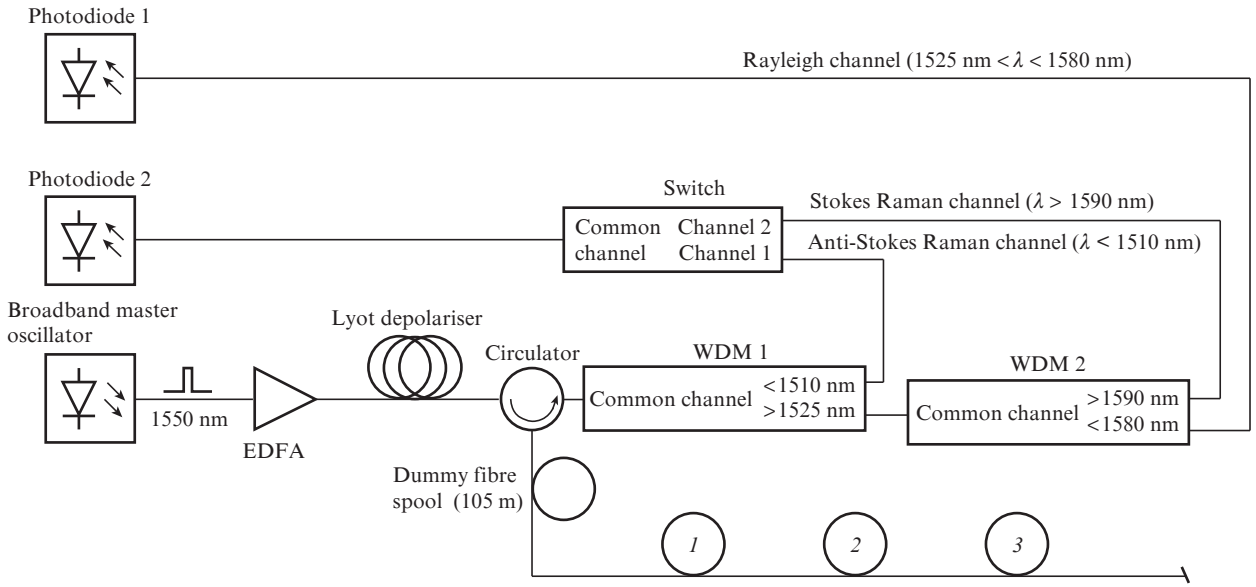

Figure 1. Schematic of the experimental setup: (EDFA) erbium-doped fibre amplifier; (WDM) wavelength-division multiplexer; (*1*) Fujikura FutureGuide-LWP fibre spool (100 m); (*2*) Corning ClearCurve XB fibre spool (90 m); (*3*) Corning SMF-28 ULL fibre spool (25 m).

fibres 100, 90 and 25 m in length, respectively, fusion-spliced in series. All three fibres had an attenuation at a wavelength of 1.55 μm in the range 0.17–0.19 dB km^{-1}. The backscattered light passed through the circulator and thin-film filters separating the Rayleigh scattering signal from the Stokes and anti-Stokes Raman signals (spectra obtained with an ANDO AQ6319 analyser are presented in Fig. 2) and entered avalanche photodiodes coupled to 50-MHz bandwidth transimpedance amplifiers. The signal was then digitised by an analog-to-digital converter (ADC) at a sampling rate of 100 MHz. The averaging time was 10 min. As a result, the signal-to-noise ratio in the Rayleigh channel reached 10^5. The spatial resolution of the reflectometer, determined by the optical pulse duration and amplifier passband, was about 1 m.

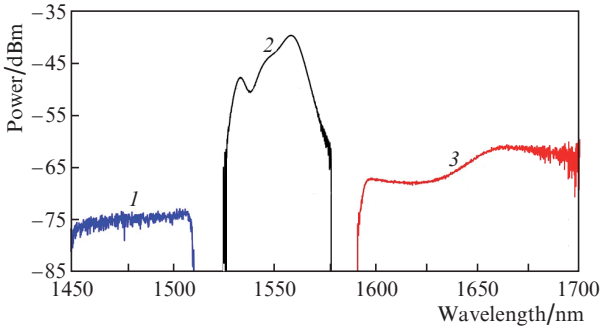

Figure 2. Optical power spectra in a 1-nm band obtained for the (*1*) anti-Stokes Raman, (*2*) Rayleigh and (*3*) Stokes Raman channels in the configuration schematised in Fig. 1.

Figure 3 shows a typical portion of Rayleigh scattering reflectograms for a Fujikura FutureGuide-LWP fibre segment. The data sets *1* and *2* were obtained with a time interval of 12 h. During this time, the temperature in the laboratory changed by 3 °C. It is seen that the hash width is 1.5%

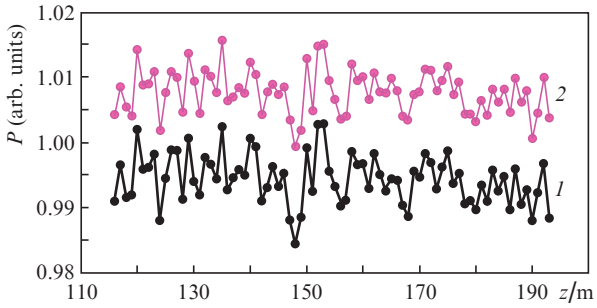

Figure 3. Portion of reflectograms (*P* is the backscattered signal power): measurements (*1*) at time zero and (*2*) 12 h thereafter.

(0.066 dB) and that the reflectograms are essentially identical in shape. The root mean square (rms) deviation calculated from the digital data for the portion of the reflectograms in Fig. 3 is 0.37% (0.016 db) in both cases.

Figure 4 shows a normalised cross-correlation function *R* constructed using the data in Fig. 3 and defined as follows:

$$R(\Delta z) = \frac{\sum_z [P_1(z) - \bar{P}_1(\Delta z)][P_2(z - \Delta z) - \bar{P}_2]}{\sqrt{\sum_z [P_1(z) - \bar{P}_1(\Delta z)]^2 \sum_z [P_2(z - \Delta z) - \bar{P}_2]^2}}, \quad (1)$$

where P_1 and P_2 are the initial signals within the z-axis intervals of interest for us; $\bar{P}_1(\Delta z)$ is the average of the P_1 signal over the overlap interval with the P_2 signal shifted by Δz with respect to P_1 along the z-axis; and $\bar{P}_2$ is the average of the P_2 signal over its own interval. The spacing between neighbouring points was 1 m. That the maximum normalised correlation coefficient approaches unity attests to a high degree of agreement between the results, and the fact that it differs from unity indirectly characterises the interference level due to the photodetector and coherence noise (the latter should show up upon temperature changes because a coherent reflectometer [2, 3] possesses extremely high sensitivity, in particular to temperature changes). From the data in Fig. 4, we can also assess

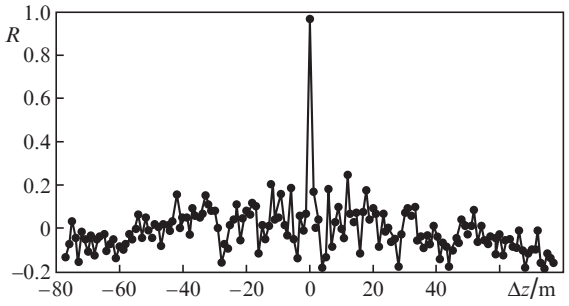

Figure 4. Normalised cross-correlation function R for the reflectograms presented in Fig. 3.

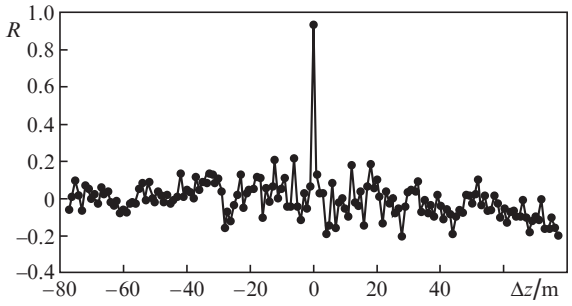

Figure 6. Cross-correlation function for two configurations differing in light propagation direction.

the correlation distance of the configurations in question: it does not exceed 1 m.

To ascertain that the noise in Fig. 3 is unrelated to residual polarisation, one, two or three turns of a 30-mm-radius fibre were rotated through 90° and fixed between sequential measurements, similarly to what occurs in a manual fibre polarisation controller. The polarisation state of light in the fibre was known to change, but no changes were detected in its reflectograms. Qualitatively similar results were obtained for the other types of fibre studied.

These data lead us to conclude that state-of-the-art telecom fibres contain inhomogeneities which cause variations in the Rayleigh backscatter coefficient. To ascertain that we deal with inhomogeneities 'frozen' in fibre, rather than with electrical cross-talk or other possible artefacts, a segment of the same fibre 5.1 m in length, which corresponded to five ADC sampling intervals, was inserted (using fusion splicing) between the circulator and test fibre. In new measurements, all inhomogeneities were shifted by five ADC sampling intervals, i.e. by about 5 m.

Figure 5 shows the autocorrelation function [calculated by formula (1) at $P_2 \equiv P_1$] and the cross-correlation function for two portions of reflectograms obtained before and after the additional fibre segment was inserted. Judging from the height of the correlation peak, there is an almost perfect coincidence of the configurations with a shift by five ADC sampling intervals, which eliminates any doubt as to the role of cross-talk in the noise contamination of reflectograms. It also follows from the autocorrelation function in Fig. 5 that the correlation distance of the inhomogeneities does not exceed 1 m, which means that neighbouring measurements made at 1-m intervals are statistically independent.

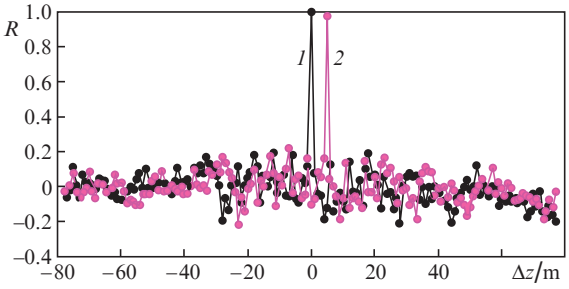

Figure 5. (*1*) Normalised autocorrelation function of an optical fibre and (*2*) normalised cross-correlation function obtained after a 5.1-m-long fibre segment was added.

We performed an additional experiment in which the opposite end of the test fibre was connected to the reflectometer. Clearly, in the presence of 'frozen-in' inhomogeneities, there should be a correlation between reflectograms in the case of longitudinal coordinate reversal. Indeed, such a correlation is clearly observed (Fig. 6). To achieve it, we had to adjust the connecting fibre length with an accuracy of 10 cm.

To explain the observed effect, two hypotheses were put forward. One of them is that, during the drawing process, the geometric dimensions of the fibre, especially the core diameter, vary. The described features of the above reflectograms should then show up as well in Raman measurements. To verify this hypothesis, anti-Stokes and Stokes signals were sequentially fed to the photodetector input. The results obtained for a 16-m-long fibre segment are presented in Fig. 7.

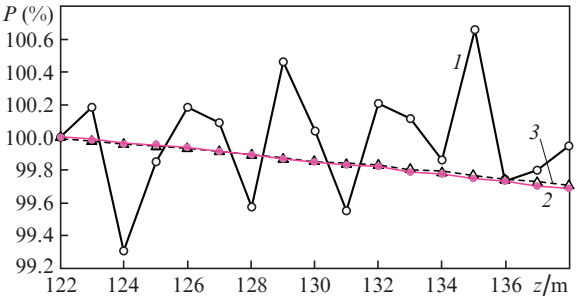

Figure 7. Reflectograms of a 16-m length of the Fujikura FutureGuide-LWP fibre for the (*1*) Rayleigh, (*2*) anti-Stokes Raman and (*3*) Stokes Raman channels.

In both cases, we detected a noiselike component, but its amplitude was considerably smaller (0.02%) than that in the case of Rayleigh scattering.

Clearly, there is no evidence in support of the former hypothesis. At the same time, it is clear from Fig. 7 that the attenuation per unit length cannot be evaluated from a Rayleigh scattering reflectogram of such small length, whereas this is rather easy to do from Raman scattering reflectograms. However, it is inadequate to evaluate optical losses from our results because our photocurrent amplifier is incapable of reproducing low frequencies, which causes the measured loss to be overestimated, but this circumstance has no effect on the main conclusions drawn in this study.

The other hypothesis is that, since noiselike behaviour is only observed in the case of Rayleigh scattering, its cause

should be sought for among its features. The Rayleigh scattering intensity is known to be determined by the scattering coefficient [6]

$$\alpha = \frac{8\pi^3}{3\lambda^4} n^8 p^2 \beta T_f, \quad (2)$$

where λ is the wavelength of the light; n is the refractive index of the medium; p is its photoelastic constant; β is its isothermal compressibility; and T_f is a fictitious temperature at which thermodynamic density fluctuations become 'frozen-in' [7]. It seems most likely that, during the fibre drawing process, the preform temperature fluctuates in the fibre formation region (at an average temperature of ~2200 K, the present results can be accounted for by variations in temperature by 2–3 K) or that the refractive index of the fused silica fluctuates by ~0.02%. It appears impossible to separately assess the contributions of these factors or estimate the influence of other effects from available data.

It is also reasonable to assume that the fibre contains inclusions or other nanoscale inhomogeneities, which have no significant effect on the key characteristics of the fibre as an information transmission medium, because their contribution to the scattering loss does not exceed 1% to 2%. In particular, such inhomogeneities determine the laser damage threshold of most optical materials [8].

Since we detected no deviations from the normal distribution law and our measurements were statistically independent, in real reflectometry, where longer probe pulses are typically used, the rms deviation of noise should be expected to decrease inversely with the square root of spatial resolution (which is proportional to the pulse duration).

The present results lead us to the following practical conclusions:

1. Since there are 'frozen-in' fluctuations in fibres, quite easy to detect and identify, individual fibres can be recognised from their signature (unique as a fingerprint) in the form of the Rayleigh scattering signal distribution, which may turn out to be useful in some applications.

2. To adequately measure the level of losses in short pieces of fibre (tens of metres), it is reasonable to detect backscattered light not at the probe wavelength but at a shifted wavelength corresponding to the Stokes Raman signal. It should then be kept in mind that the Raman scattering intensity is temperature-dependent and that, without taking into account this circumstance, one can deal with loss measurements only at a constant temperature throughout the length of the test fibre.

3. The observed variations in the Rayleigh backscatter coefficient, due to the presence of structural inhomogeneities, should be taken into account in designing distributed physical parameter sensors using Rayleigh scattering intensity as a reference channel.

3. Conclusions

Considerable 'frozen-in' Rayleigh scattering coefficient fluctuations have been found in telecom single-mode optical fibres by reflectometry. Measurements were performed at a wavelength of 1560 nm (C band). At a 1-m spatial resolution of the reflectometer used, the hash width for the Fujikura FutureGuide-LWP fibre is 0.066 dB, the standard deviation is 0.016 dB, and the correlation distance of the inhomogeneity distribution along the length of the fibre does not exceed 1 m. These values determine the accuracy achievable in measurements of the attenuation coefficient of fibres with optical reflectometers, and this should be taken into account in designing distributed sensors using Rayleigh scattering intensity as a reference channel. We have discussed possible sources of the inhomogeneities.

References

1. Gorshkov B.G. et al. RF Patent No. 2 552 222 (2011).
2. Brinkmeyer E., Streckert J. *J. Lightwave Technol.*, **4**, 513 (1986).
3. Avdeev B.V., Morgunov D.Yu., Treshchikov V.N. *Foton-Ekspress*, (2), 25 (2004).
4. Gorshkov B.G., Paramonov V.M., Kurkov A.S., Kulakov A.T. *Lightwave Russ. Ed.*, (4), 47 (2005).
5. Gorshkov B.G., Paramonov V.M., Kurkov A.S., Kulakov A.T., Zazirnyi M.V. *Kvantovaya Elektron.*, **36**, 963 (2006) [*Quantum Electron.*, **36**, 963 (2006)].
6. Pinnow D.A. et al. *Appl. Phys. Lett.*, **22**, 527 (1973).
7. Sakaguchi S. et al. *J. Non-Cryst. Solids*, **220**, 178 (1997).
8. Manenkov A.A., Prokhorov A.M. *Usp. Fiz. Nauk*, **148**, 179 (1986).